

# **ETCHED TRACK DETECTORS**

---

## **2.1 Historical Review**

Wilson's observation of individual alpha particles tracks in supersaturated moist air in 1898 laid down the basis for the track technique. In his cloud chamber, a string of microscopic water droplets was formed along the particle track that was triggered by the secondary ions created along the path of an alpha particle (Durrani and Bull, 1987). This rapidly fading phenomenon revealed a direct preview of the atomic domain.

Sixty years later, in 1958, Young observed etched tracks of fission fragments in the solid phase (i.e. LiF) but probably saw no future in pursuing the object. In 1959, Silk and Barnes observed hair like unetched latent tracks of fission fragments in mica using Transmission Electron Microscope (TEM). Since the latent tracks faded and were lost in the electron beam of the TEM, these workers too dropped the idea of further work on the subject as they felt difficulties in using this methodology (Fleischer, 1998). During early 1960s the team of Walker, Fleisher and Price saw Silk and Barnes work and extended the etching technique of Young to mica, glasses, plastics and mineral crystals. The initial applications of damage track detectors to a number of fields stem from the work of this team, who pioneered the extensive development of these detectors (Fleischer et al., 1975; Durrani and Bull, 1987).

Since its inception, Solid State Nuclear Track Detectors (SSNTDs) have found remarkable applications in nearly all branches of science and technology. These applications include studies in nuclear physics, radiography, cosmic rays, dosimetry, environmental science, geosciences, indoor radon measurement, earth sciences and mineral exploration (Fleischer et al., 1975). The simplicity and low cost of this detection technique have led to extensive research in the field of (SSNTDs). Developments in this field are reported in many journals including the journal of Radiation Effects and Defects in Solids, Radiation Measurements, Nuclear Instruments and Methods in Physics Research, Health Physics, Applied Physics, etc.

The basic principle of application of track detectors is based on the fact that the passage of a heavily ionizing charged particle through a solid insulator creates

microscopic trails of radial damage along its path. These latent tracks can be visualized in various ways following a suitable treatment, such as chemical etching. Particle tracks are formed in many insulating materials but not in conductors or semiconductors. The classification of track-storing and non-track-storing materials depends on electrical resistivity. Materials with values greater than  $\sim 2000 \Omega\text{-cm}$  generally store tracks (Durrani and Bull, 1987).

## 2.2 Advantages of SSNTDs

The main advantages of SSNTDs are following.

- Relatively inexpensive.
- They are sensitive to radiations of high linear energy transfer (LET) but are insensitive to beta rays, gamma rays and x-rays. .
- Ease of development (there is no need for darkroom as in the case of nuclear emulsions). Simple chemicals (e.g. NaOH, KOH) are used in ordinary day light to etch and make visible tracks in polymers/ mineral crystals/ glasses.
- They are 'integrating devices' and produce a cumulative record over a period of time.
- Permanent record of measured exposure (unlike TL where the read-out destroys the record).
- Track recorded in geological and extraterrestrial samples (meteorites) remain intact for millions, indeed billions, of years.
- They are passive detectors and do not require power supplies during its use, in contrast to electronic detectors such as ionization chambers.
- Heavily charged particles (such as fission fragments) can be distinguished from lighter charged particles e.g. alpha particles.
- Some of SSNTDs e.g. CR-39 can detect charged particles down to protons.
- They are small, durable and thus can be used in homes for indoor radon measurements as well as in application where small geometry is important.

## 2.3 CR-39 Polymeric Track Detectors

CR-39 (Columbia Resin-39) is the trade name of the thermoset plastic which is a polymeric form of diethylene glycol bis (allyl carbonate). Its simple formula is  $(C_{12}H_{18}O_7)_n$ . It has widespread commercial use as it is very transparent and

mechanically rigid. Although CR-39 was already in use for multiple purposes (e.g. in sun glasses, wind screen of aero planes, etc.), its excellent nuclear track recording properties were reported in 1978 by Cartwright et al. Plastic detectors may be characterized by a threshold value of  $dE/dx$ , above which etchable tracks are formed in a given material. CR-39 is very sensitive to ionizing radiation and has the lowest  $dE/dx$  threshold of any known SSNTDs. CR-39 can detect protons of energy up to 10 MeV in energy and has a wide range (several tens of MeV) for  $\alpha$ -particles detection (see Table 2.1) (Durrani and Bull, 1987). CR-39 offers many advantages over its rivals. It is highly isotropic, homogenous, relatively stable to environmental conditions (unlike, say, LR 115) and there is no cross linking after radiation damage has broken the chemical bonds. Much-work has been done to study properties of CR-39 (Al-Najjar and Durrani, 1984; Green et al., 1982) confirming that it is a desirable solid state nuclear track detector. CR-39 is now in use in many fields of Science and Technology that include the personnel neutron dosimetry, radon dosimetry, etc. (Matiullah, 2000).

The track recording efficiency of CR-39 also depends on the processing conditions and can be modified, to some extent, by the processing conditions adopted. This includes etchant type, strength, temperature, and etching time. Extensive work has been done to optimize the etching conditions using NaOH and KOH (Durrani and Bull, 1987). In this direction I have made further progress and have discovered new efficient etchants which are presented in the preceding chapter.

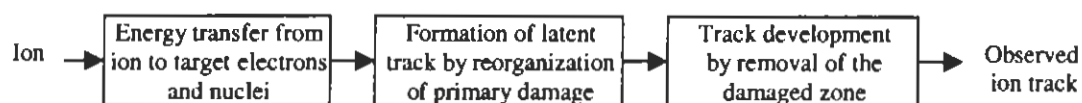
**Table 2.1:** Limits of detectable  $\alpha$ -particle energies for some plastic\*

Type of plastic	$E_{min}$ (MeV)	$E_{max}$ (MeV)
Lexan and Makrofol E polycarbonates	~ 0.2	~ 3
Cellulose nitrate (CA 80-15; CN 85; LR 115; Daicel)	~ 0.1	4-6
CR-39 (allyl diglycol carbonate)	~ 0.1	> 20

\* The upper and lower  $\alpha$ -energy limits are intended as rough guide only. They depend on the etching conditions and on the exact form of the plastic used. In the case of polycarbonates, post irradiation exposure to U.V. light facilitates the revelation of  $\alpha$ -particle tracks.

## 2.4 Formation of the Latent Tracks

Under what circumstances is an etch-able track formed? To answer this question one must understand the following three-step approach of track creation.



On its way through the solids the projectile-ion loses its energy in terms of  $dE/dx$  during ionization and excitation processes. As a result of the primary ionization occurring along the projectile-ion trajectory, an ion cloud remains along the projectile trajectory. The corresponding electrons are emitted to large distances from the projectile trajectory producing electronic collision-cascades (Delta rays). Due to coulomb repulsion the ion cloud will expand explosively resulting in the atomic collision-cascade. As a result of the electronic and atomic collision-cascades, a cloud of interstitial atoms and vacancies is formed in the close vicinity of the ion trajectory. In inorganic solids the minimum energy of an atom to be removed from its original site and be displaced to another site (i.e. displacement energy) is of the order of 10–15 eV. On the other hand the organic plastic detectors being made of long chain molecules, the energy required to break the chain is considerably low i.e. 2–3 eV. Chain break, in turn, lowers the molecular weight and allows more rapid chemical attack. The detection sensitivity of plastic detectors is correlated to the ease of producing chain breaks.

Ultimately the atomic defects reorganize to form the track core of about 0.01  $\mu\text{m}$  diameter along the projectile-ion path. Further away, at larger distances from the ion trajectory, the electronic collision-cascade leads to excited atoms and molecules and free radicals are formed, as secondary chemical reactions. The main features of the formation of the track core may briefly be described with the help of following two models.

## **2.4.1 Models of Track Formation**

### **2.4.1.1 Thermal-Spike Model**

The energy loss mechanism of the projectile-ion leads to electronic and atomic collision-cascades. The atomic collision-cascade deposits its energy in the close vicinity of the ion trajectory, while the electronic collision-cascade has long range so its thermal effects can be neglected. The thermal spike model simplifies the complex effects of the atomic collision-cascade by assuming a simple thermal distribution. According to the thermal spike model the deposited energy corresponds to an abrupt temperature rise in a small cylindrical volume around the ion trajectory at the time of passage  $t=0$ . After the passage of the ion i.e. for  $t>0$ , the thermal energy diffuses away from the ion trajectory. The thermal spike creates defects via thermal activation which are remaining as 'frozen defects' along the ion trajectory due to the rapid

quenching of the temperature. If  $\alpha$ -particle deposits an energy  $Q$  per unit path length at time  $t = 0$ , then the temperature  $T$  as a function of  $t$  and of radial distance,  $r$ , from the axis of the ion path is given by:

$$T(r,t) = T_0 + \frac{Q}{4\pi cdDt} \exp\left(-\frac{r^2}{4Dt}\right) \quad (2.1)$$

Where  $T_0$  is the initial temperature of the lattice,  $c$  is the heat capacity of the medium,  $d$  is its density and  $D$  is the thermal diffusivity. If it is assumed that a high temperature is maintained (many thousands of degrees Kelvin for a short time for an incident fission fragment), processes such as melting and recrystallization would occur and thus point defects (e.g., vacancies and interstitials) would be highly probable (Chadderton et al., 1993). For all this to happen, the heat conductivity in the material should be low. This explains the inability of metals to show etchable tracks as the thermal spike becomes too broad and diffuses in the metal lattice, whereas in insulators, a narrow, intense spike is produced. This leads to sufficient localized radiation damage capable of producing etchable tracks.

#### 2.4.1.2 Ion-Explosion Spike Model

The mechanism for latent track formation based on ion explosion spike model is depicted in Fig. 2.1. This model was proposed by Fleischer et al., 1975. According to this model, a charged particle passing through the insulating material results in a high concentration of positive ions along its path due to coulomb interaction. If the recombination time is long compared with the lattice vibration time ( $\sim 10^{-13}$  s) the positive ions may repel each other, driving the ions into interstitial positions and leaving behind a vacancy-rich cylindrical core. Thus, a cylinder of 4–8 nm diameter and a few mm long is formed, which could be seen under transmission electron microscope. If it is chemically enlarged then the etched tracks may be seen under an optical microscope. According to this model, the requirements for track formation are that: (a) the electrostatic stress (i.e. the Coulomb repulsive forces within the ionized region) should be greater than the mechanical strength or lattice-bonding forces, which implies that materials of low mechanical strength or low dielectric constant are more likely to store etchable tracks; (b) The maximum permissible density of free electrons  $n_f$  must be low. This condition restricts track formation to good insulators and excludes metals; (c) tracks will not be formed in materials having high hole

mobility, the reason being that a rapid outward diffusion of holes will neutralize the core atoms, which in turn will inhibit formation of tracks. Thus, semiconductors like silicon and germanium, which have a high hole mobility, will not record tracks. This model is currently the most widely accepted in the tracks field, although it is quite possible that some combination of the models could give a more accurate picture of the actual method by which nuclear tracks are formed in solids.

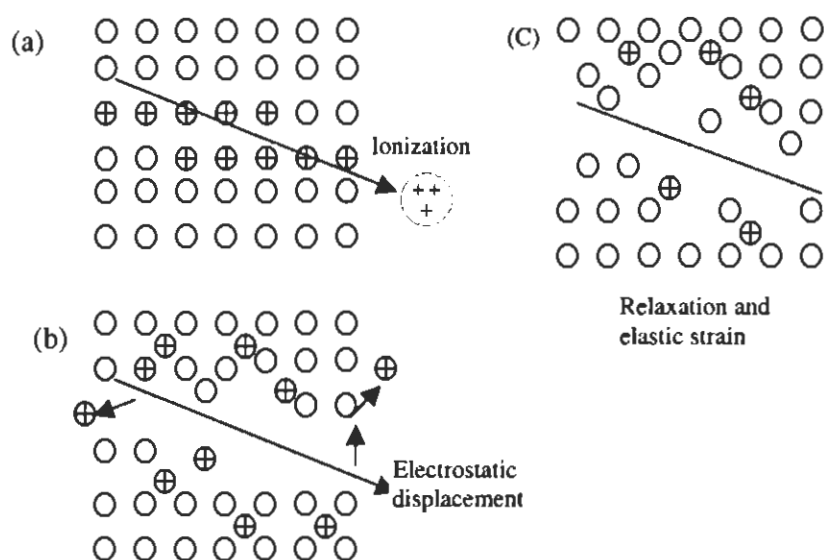


**Figure 2.1:** *The ion explosion spike mechanism for track formation in inorganic solids: The original ionization left by the passage of a charged particle (a) is unstable and ejects ions in to the solid, creating vacancies and interstitials (b). Later, the stressed region relaxes elastically (c) Straining the undamaged matrix (after Fleischer et al., 1975).*

## 2.5 Track Formation in Polymers

In organic polymers, the passage of heavily charged particles results in scissions or a number of broken polymer chains (see Fig. 2.2). A thermal spike (see Section 2.4.1.1) along the trajectory of the charged particle causes localized melting and, this, together with excitation, leads to chain-breaking and production of new chain ends. Chemically reactive sites are formed at the points of scission, which may be enlarged when an etchant such as NaOH enters the damaged region by dissolving the distorted and degraded portions. According to Durrani and Bull, 1987, in plastics, ionized and excited molecules and electrons are produced by ionizing radiations. Excitation energy can be transferred from one molecule to another. Electrons may be trapped at

various sites and may combine with molecules to form negative ions, or they may recombine with positive ions yielding excited molecules. Both ions and excited molecules may acquire considerable vibrational energy and undergo bond rupture to form a complex array of stable molecules, free radicals and ionized molecules. The net effect on the plastic will be the production of many broken molecular chains and production of a damaged region known as a latent track, leading to a reduction in the average molecular weight of the polymers.

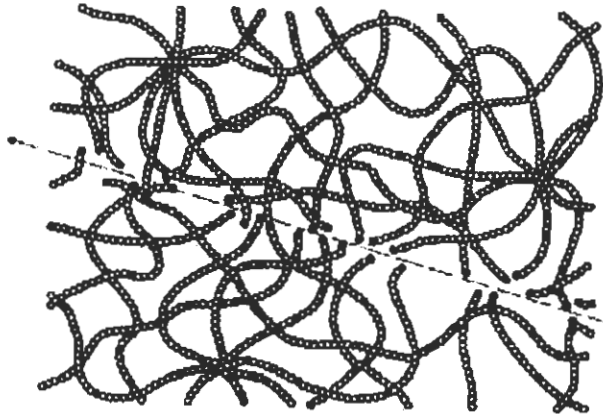


**Figure 2.2:** Schematic diagram of chain scission in polymers caused by the passage of heavily charged-particles.

A theory for latent particle tracks in polymers was given by Chadderton, et al. The model accounts generally for the evolution of intrinsic radiation damage zones in a polymer. The number of broken bonds,  $n_b$ , is, given by;

$$n_b = f A_i R_p V_b \quad (2.2)$$

Where  $f$  denotes the probability for a bond to be ruptured for a given energy transfer from the projectile at a given depth and is assumed constant;  $A_i$  is an average cross-sectional area of a latent track produced by a given ion entering a polymer surface perpendicularly;  $R_p$  is the average length of a latent track; and  $V_b$  is the average number of bonds per unit volume.

To summarize, latent tracks in polymers produced by charged particles are due to the chemical bond-breaking events along the trajectories. Ion-beam induced scission of polymeric chains typically produces charge redistribution along the skeletal backbone of a polymer molecule. This, in turn, gives rise to chemically unsaturated bonds and a variety of topological cross-linking rearrangements of

polymer's molecular fragments. Owing to the lower average molecular weight of matter in the latent track, the etchant preferentially attacks this region and converts it into a visible etched track by performing chemical etching procedures which are briefly described in the next section.

## **2.6 Development of Latent Tracks in Polymers**

During the track development, damaged zone of the latent track is chemically transformed or removed by an etchant that leads to an observable etched track. The evolution of track shape during the etching process depends mainly on the ratio of track etch rate  $V_T$  and bulk etch rate  $V_B$ . In the following sections chemical etching and track etch geometry is discussed.

### **2.6.1 Chemical Etching**

This is the most common method used for enlarging the size of the latent tracks produced by heavily ionizing particles. Chemical etching is usually carried out in a thermostatically controlled bath at temperatures ranging from 30 °C to 80 °C. The etching time is 2–16 h. Different etchants are used for different detectors. The etchants which have been most commonly used for plastic detectors are aqueous alkaline solutions of NaOH and KOH with concentrations of 1 to 12 M. For example, for standard 6 M NaOH solution, 240 g of NaOH is added into distilled water such that total solution becomes one liter. The size of track depends upon the concentration of etching solution, etching time and temperature.

In order to etch the detectors, an elastic spring (holding many detectors) is attached to a wire and immersed in to the etching solution within a beaker. The top of the beaker is covered with a glass lid to avoid evaporation. The beaker is then placed in a temperature controlled water bath. At the end of the etching, the detectors are removed and washed under running tap water, to remove the etching residue from the etch pits. After drying, the detectors are counted under an optical microscope. The etched track diameters are typically a few  $\mu\text{m}$  in size and grow larger in size after prolonged etching.

Chemical etching works on the principle that once a material is placed in a suitable etchant, the solution preferentially attacks the damaged core of the track and penetrates along its length with a velocity  $V_T$  while, the surrounding undamaged material is attacked at a lower rate of  $V_B$ , the bulk etching velocity.  $V_B$  is generally

constant for given etching conditions, whereas  $V_T$  depends on the amount of damage present in the region of the core (i.e. on the nature of the ionizing particle), and will usually vary along an individual track.

The detector's track registration efficiency largely depends on the; (a) composition and concentration of the chemical etchant (b) temperature and (c) etching time. The efficiency of CR-39 detector etched for 8h at 70 °C in conventionally used 6 M aqueous solution of NaOH is 64% (for  $\alpha$ -particle from  $^{252}\text{Cf}$  in 2 Pi geometry). In order to improve the etching efficiency of CR-39, some more efficient etchants have been discovered that will be discussed in detail in the next chapter.

### 2.6.2 Mathematical Details of Track Formation

Nuclear particles incident on a track detector may be characterized by their charge  $Z$  (or effective charge  $Z_{\text{eff}}$ ), mass  $M$ , and energy  $E$  (or relative velocity,  $\beta = v/c$ ). Differences in these particle parameters manifest themselves as changes in the track length  $R$  and the track etching rate  $V_T$  as well as in the variation of  $V_T$  with position along the track. The most easily measurable parameters of an etched track are the etched-cone length  $L_e$  or the length  $S$  projected onto the detector surface and the major and minor axes  $D, d$  of the etch pit opening (see Figs. 2.3 and 2.4). The main purpose of this topic is to relate these latter parameters to the track and bulk etch rates  $V_T$  and  $V_B$  and to the track length  $R$  (I shall use  $R$  in the treatment that follows to denote the length of the damage trail in the detector, whereas  $L_e$  will refer to the length of the conical etched-out track). The track etching geometry also determines quantities such as the efficiency of a given detector which is defined as the ratio of the number of observed etched tracks to the number of latent damage trails crossing a unit area of the "original" surface of the detector (i.e. where the etching first starts).

In the remainder of this section, some of the general features of track etching geometry are indicated. Some of the simpler derivations are also presented.

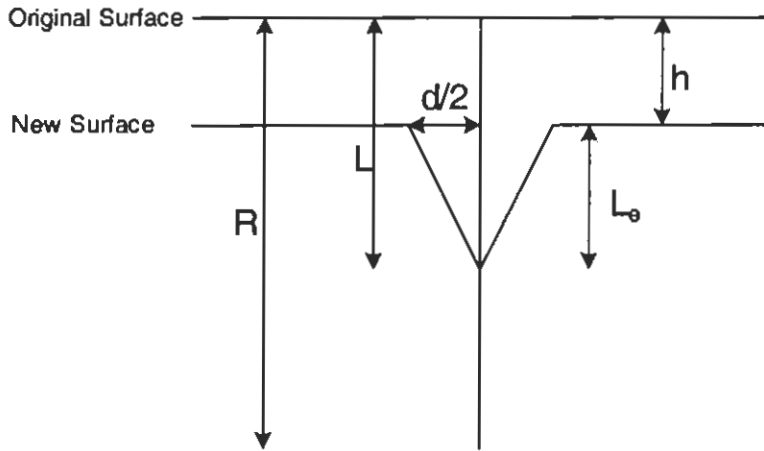


**Figure 2.3:** Some parameters used to describe the geometry of the etched tracks.

Some parameters that are used to describe the geometry of etched tracks are shown in Fig. 2.3. As may be seen in this figure,  $R$  = full length of the latent track;  $L$  = length of track attacked by the etchant up to a given moment;  $L_e$  = observed length of the etched track;  $h$  = thickness of surface removed by etching;  $d$  = diameter of the etch-pit opening.

### 2.6.2.1 Constant Track Etching Velocity, $V_T$

The calculation of etched-track parameters is comparatively simple when the track etch rate  $V_T$  is taken to be constant. This condition will apply in many instances where the ionization rate of the particle is not varying rapidly such as the case of an energetic cosmic-ray nucleus. Furthermore, the constant  $V_T$  model allows a number of features of the track etching process to be established fairly simply.

Initially, some further simplification shall be made by concentrating on a track which is normally incident upon the detector surface (Durrani and Bull, 1987). Now, the linear rate of attack down the track is  $V_T$  (the radial extent of the enhanced etchability is assumed to be very small compared with the final dimensions of the etched track), so that in an etching time,  $t$ , the etch pit will extend to a distance  $L$  from the point of origin, where  $L = V_T t$ . However, the surface is also being removed at a rate  $V_B$ , so that the length of the etch pit is

$$L_e = V_T t - V_B t \quad (2.3)$$

At each point along the track, the etchant moves outwards at a rate  $V_B$ . Any point at a distance,  $y$ , from the beginning of the track is reached by the etchant at a

time  $t(y) = Y/V_T$  and there is a residual time  $t - t(y)$  available for the etchant to attack radially outwards from the point at  $y$  to a distance  $V_B \times (t - t(y))$  in the medium. The three-dimensional pit wall is then formed by the locus of all the spheres of radius  $V_B \times (t - t(y))$ , where  $t(y)$  is the variable. It will be seen from Fig. 2.4 that this leads to the formation of a cone with semi-cone angle  $\delta$  given by

$$\sin \delta = \frac{V_B t}{L} = \frac{V_B t}{V_T t} = \frac{V_B}{V_T} \quad (2.4)$$

This angle  $\delta = \sin^{-1} \left( \frac{V_B}{V_T} \right)$  is also known as the critical angle of etching ( $\theta_c$ ). From the triangle O'PT in Fig. 2.4, it is apparent that

$$\frac{d/2}{L_e} = \tan \delta \quad (2.5)$$

From Eq. (2.4) it follows that

$$\tan \delta = \frac{V_B}{\sqrt{V_T^2 - V_B^2}}$$

So that, from Eq. (2.5),

$$d = \frac{2V_B L_e}{\sqrt{V_T^2 - V_B^2}}$$

Using the value of  $L_e$  from Eq. (2.3) we then obtain

$$d = \frac{2V_B (V_T - V_B)}{\sqrt{V_T^2 - V_B^2}}$$

or 
$$d = 2V_B t \sqrt{\frac{(V_T - V_B)}{(V_T + V_B)}} \quad (2.6)$$

Some features of track etching have emerged from this simple calculation, which are in fact found to apply in more general cases.

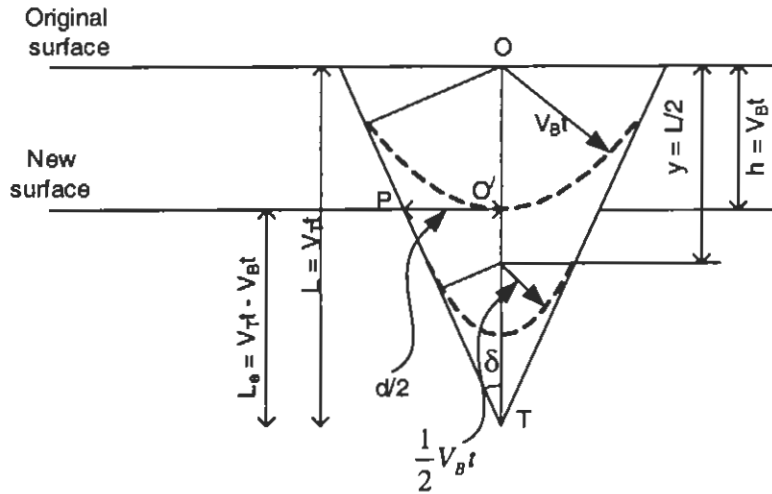


**Figure 2.4:** Construction for the calculation of etched-track parameters for a track of constant  $V_T$ , lying normally to the detector surface. The semi-cone-angle is denoted by  $\delta$  ( $=$  critical angle,  $\theta_c$ ); the other parameters are as explained in the caption to Fig. 2.3.

- (1) The semi-cone angle  $\delta = \sin^{-1} (V_B/V_T)$ . In certain materials such as glasses where  $V_T$  is not very much greater than  $V_B$ , etched tracks with large cone angles are produced. In plastics and minerals, long needle-like tracks of much smaller cone angle are usually produced. This is a consequence of the fact that  $V_T \gg V_B$  in these cases.
- (2) The diameters of the surface openings of etched tracks increase with increasing  $V_T$ , reaching a maximum of  $2V_B t$  when  $V_T \gg V_B$  (see, Eq. (2.6)).

### 2.6.2.2 Calculation of Major and Minor axes and $L_e$

Having performed calculations for normal incidence case,  $D, d$  (the major and minor axes of the opening, respectively) and  $L_e$  can be easily calculated for a track incident at some arbitrary dip angle  $\theta$  with the detector surface (see, Fig. 2.5). The track opening being the intersection of a cone with a plane surface making an angle  $\theta$  with the axis of the cone, the resulting shape is a conic section: an ellipse, in fact, with major axis  $D$  and minor axis  $d$  (For a normally-incident track,  $D = d$ ).

The length of the etch pit,  $L_e$ , as measured from the cone tip to the point where the damage trail crosses the final etched surface of the detector, is now  $V_T t - (V_B t/\sin\theta)$ . Note that this point of intersection  $O'$  no longer divides  $D$  into two equal portions. After some lengthy calculations, it can be shown that (Durrani and Bull, 1987).

$$D = \frac{2V_B t \sqrt{V_T^2 - V_B^2}}{V_T \sin \theta + 1} \quad (2.7)$$

An alternative expression for Eq. (2.7) is obtained, by putting  $V = V_T/V_B$ , as

$$D = \frac{2V_B t \sqrt{V^2 - 1}}{V \sin \theta + 1} \quad (2.8)$$

The expression for minor axis  $d$  of the track opening, come out to be (Durrani and Bull, 1987).

$$d = 2V_B t \sqrt{\frac{V \sin \theta - 1}{V \sin \theta + 1}} \quad (2.9)$$

A further important feature of track etching is revealed by this last equation when  $\theta$  assumes a value such that  $V \sin \theta = 1$ , then  $d$  vanishes and for all lower values of  $\theta$ ,  $d$  is imaginary. The reason for this is that when  $V \sin \theta = 1$ , the component of the track etch velocity normal to the surface is equal to the bulk etch velocity, so that the tip of the etch cone never keeps ahead of the advancing surface. The track therefore is never observable. As mentioned earlier, the angle  $\theta_c$ , defined by  $\sin \theta_c = 1/V = V_B/V_T$ , is known as the critical angle of etching, and represents the minimum angle to the surface that a track can make in order to be revealed by etching. It will be seen that  $\theta_c = \delta$ , the semi-cone-angle (see Eq. (2.4)).

### 2.6.2.3 Determination of Track Parameters $R$ and $V_T$

Among the most important parameters of the latent damage trail which are often required to be determined are the length  $R$  and the mean value of the track etch velocity  $V_T$ . It is relatively easy to measure the track parameters  $S$ ,  $D$ , and  $d$  by using a micrometer attachment to the microscope eyepiece or from a photomicrograph/video screen projection.  $V_B$  can also be measured from the changes in the thickness of the plastic or the glass sheet. It may be noted here that thickness method can not be applied to CR-39 detector because irreversible swelling take place in the case of CR-39 detector at elevated temperatures. Alternatively, sheet of plastic is irradiated with  $^{252}\text{Cf}$  fission fragments at normal incidence. Then, for  $\theta = 90^\circ$ ,

$$D = d = 2V_B t \sqrt{\frac{V-1}{V+1}} \quad (2.10)$$

Where  $V = V_T/V_B$ . Since for most plastics and etching conditions used the track etch rate for fission fragments is very much higher than the bulk etch rate (so that  $V \gg 1$ ), we have

$$D = d \cong 2V_B t$$

$$V_B \cong \frac{D}{2t} \quad (2.11)$$

Thus a measurement of the diameter of the normally incident fission-fragment tracks at a known etching time yields a value for the bulk etch rate. If the ratio of the diameters of some tracks (having an etch rate ratio  $V$ , say for alpha particle) to those of fission fragments is denoted by  $x$ , then we can write (using Eqs. (2.10) and (2.11))

$$x = \sqrt{\frac{V-1}{V+1}}$$

and upon re-arranging, we get the useful formula

$$V = \frac{1+x^2}{1-x^2} = \frac{V_T}{V_B} \quad (2.12)$$

OR

$$V_T = V_B \left( \frac{1+x^2}{1-x^2} \right) \quad (2.13)$$

Most treatments of track geometry are formulated directly in terms of the thickness of the removed surface layer  $h = V_B t$ .

## 2.7 Etch Pit Profile with Prolonged Etching

Figure 2.6 shows the evolution of an etch pit profile with prolonged etching. The track shown in this figure has  $V (= V_T/V_B) = 2$ , and makes a dip angle  $\theta = 70^\circ$  with the detector surface  $O$ . As may be seen in this figure, the track profile goes through three phases:

- (1). The conical phase: in this phase the latent track is not fully etched. The etching proceed at the track etch rate,  $V_T$ .
- (2). Transition phase: After the latent tack is fully etched, the etching takes place at the rate of  $V_B$ .



## 2.8 Track Counting

The most common method of track counting employs an optical microscope, with a grid in its eyepiece. After several hours chemical etching, the etched tracks have diameters of several micrometers. An ordinary microscope with an objective magnification of 40 may be adequate to count these tracks. However, field of view (FOV) of the microscope has to be calibrated against a standard graticule for the objective magnification which is used for counting.

Alpha particles emitted from radon atoms in air may originate at any point at a distance equal to the range of alpha particle and may fall on the detector surface at any angle. Consequently, the sizes and shapes of tracks will be different as shown in Fig. 2.7. This figure shows etched tracks in radon-exposed CR-39 detector in a closed container and etched for 16 h in 6 M NaOH at 80 °C.

Surface artifacts will also be enlarged upon etching and have to be distinguished from the genuine tracks which may be identified by slowly moving the fine focus of the microscope up and down. From the bright point of the internally reflected light at the bottom tip of the etch-pit cone, a genuine etched pit may be distinguished from the artifact because it has a well-defined geometric shape (with a circular or elliptical mouth-opening at the detector surface). A controlled (i.e. unexposed) CR-39 detector is simultaneously etched with radon-exposed detectors in order to find out the background tracks. A total few hundred tracks counted over a number of fields of view are usually considered to yield reasonable statistics. The track density is obtained using the following relation.

$$\rho = \frac{\sum_i N_i}{nA} \quad (2.14)$$

Where  $N_i$  is the total number of tracks counted in the  $i$ th field of view,  $A$  is the area of the field of view under the magnification used and  $n$  is the total number of fields of view.

The statistical error in counting can be estimated by the square root of the total number of tracks actually counted (Durrani and Bull, 1987):

$$\sigma_\rho = \frac{\sqrt{\sum N}}{nA} \quad (2.15)$$

For example if one counts 400 tracks, the standard error is  $(400 \pm \sqrt{400}) / nA$ .



**Figure 2.7:** *Tracks Revealed on CR-39 exposed to radon in a closed chamber and etched in 6M NaOH at 80 °C for 16 h.*

## 2.9 References

- Al-Najjar, S.A.R. and Durrani, S.A., 1984. Track profile technique and its applications using CR-39. I:-Rang and energy measurements of alpha-particles and fission fragments; II: Evaluation of V versus residual range. *Nucl. Tracks*, 8, 45–49 (I) and 51–56 (II).
- Cartwright, B.G., Shirk, E.J. and Price, P.B., 1978. CR-39: A nuclear track recording polymer of unique sensitivity and resolution. *Nucl. Instrum. Meth.*, 153, 457–460.
- Chadderton, L.T., Cruz, S.A., and Fink, D.W., 1993. Theory for latent particle tracks in polymers. *Nucl. Tracks Radiat. Meas.*, 22, 29–38.
- Durrani, S.A. and Bull, R.K., 1987. *Solid State Nuclear Track Detection: Principles and Applications*. Pergamon Press, Oxford.
- Eng, W., 1980. Introduction to plastic nuclear track detectors. *Nucl. Tracks*, 4, 283–308.
- Fleischer, R.L., 1998. *Tracks to Innovation*. Springer-Verlag New York, Inc.
- Fleischer, R.L., Price, P.B. and Walker, R.M., 1975. *Nuclear Tracks in Solids: Principles and Applications*, University of California Press, Berkeley.
- Green, P.F., Ramli, A.G., Al-Najjar, S.A.R., Abu-Jarad, F. and Durrani, S.A., 1982. Studies of bulk-etch rates and track-etch rates in CR-39. *Nucl. Instrum. Meth.*, 203, 551–559.
- Khan, H.A. and Qureshi, A.A., 1994. Solid State Nuclear Track Detection: A Useful Geological/Geophysical Tool. *Nucl. Geophys.*, 8, 1–37.
- Durrani, S.A. and Bull, R.K., 1987. *Solid State Nuclear Track Detection: Principles and Applications*. Pergamon Press, Oxford.
- Matiullah, 2000. *Radiation Physics*. Published by Allama Iqbal Open University, Islamabad, Pakistan.